JACS
JOURNAL OF THE AMERICAN CHEMICAL SOCIETY

Communication

pubs.acs.org/JACS

Evidence for an Alternative to the Oxygen Rebound Mechanism in C–H Bond Activation by Non-Heme $Fe^{IV}O$ Complexes

Kyung-Bin Cho,[†,§] Xiujuan Wu,[†,§] Yong-Min Lee,[†] Yoon Hye Kwon,[†] Sason Shaik,*[,‡] and Wonwoo Nam*[,†]

[†]Department of Bioinspired Science and Department of Chemistry and Nano Science, Ewha Womans University, Seoul 120-750, Korea

[‡]Institute of Chemistry and The Lise Meitner-Minerva Center for Computational Quantum Chemistry, The Hebrew University of Jerusalem, 91904 Jerusalem, Israel

Supporting Information

ABSTRACT: The hydroxylation of alkanes by heme $Fe^{IV}O$ species occurs via the hydrogen abstraction/oxygen rebound mechanism. It has been assumed that non-heme $Fe^{IV}O$ species follow the heme $Fe^{IV}O$ paradigm in C–H bond activation reactions. Herein we report theoretical and experimental evidence that C–H bond activation of alkanes by synthetic non-heme $Fe^{IV}O$ complexes follows an alternative mechanism. Theoretical calculations predicted that dissociation of the substrate radical formed via hydrogen abstraction from the alkane is more favorable than the oxygen rebound and desaturation processes. This theoretical prediction was verified by experimental results obtained by analyzing iron and organic products formed in the C–H bond activation of substrates by non-heme $Fe^{IV}O$ complexes. The difference in the behaviors of heme and non-heme $Fe^{IV}O$ species is ascribed to differences in structural preference and exchange-enhanced reactivity. Thus, the general consensus that C–H bond activation by high-valent metal–oxo species, including non-heme $Fe^{IV}O$, occurs via the conventional hydrogen abstraction/oxygen rebound mechanism should be viewed with caution.

High-valent $Fe^{IV}O$ species are ubiquitous in nature and perform a wide range of important chemical and biological reactions.[1] In heme enzymes such as cytochrome P450, $Fe^{IV}O$ porphyrin π-cation radical intermediates, called compound I (Cpd I), are known to perform a variety of oxygenation reactions, including alkane hydroxylation.[2] It has been shown in both experimental and theoretical studies that alkane hydroxylation by Cpd I is initiated by a rate-determining hydrogen abstraction step by the $(Porp^{\bullet+})Fe^{IV}O$ species (Scheme 1A, pathway a), which is followed by an oxygen rebound step between the resulting $(Porp)Fe^{IV}OH$ and substrate radical species (Scheme 1A, pathway b).[2] The oxygen rebound mechanism has been strongly supported and is well-established in enzymatic reactions using a special group of substrates termed "radical clocks"[2c] as well as in biomimetic iron–oxo porphyrin reactions.[3,4]

In non-heme iron enzymes and models, C–H bond activation of alkanes by non-heme $Fe^{IV}O$ species has been proposed to give alcohol products via the hydrogen abstraction/oxygen rebound mechanism (Scheme 1B, pathways a and b).[5−7] In addition, non-heme $Fe^{IV}O$ intermediates occasionally produce desaturated products (Scheme 1B, pathways a and c).[8,9] In these hydroxylation/desaturation reactions, Fe^{II} species are presumed to be the end product.[5−9] Indeed, theoretical calculations have found a small barrier for the oxygen rebound and desaturation reactions by the Fe^{III}–OH species.[7,9] Moreover, since hydroxylated/desaturated products are usually detected in experiments, there seemed to be no doubt that non-heme $Fe^{IV}O$ species follow the heme $Fe^{IV}O$ paradigm (e.g., the hydrogen abstraction/oxygen rebound mechanism). However, several recent reports do not fit into this picture. For example, it has been shown that two $Fe^{IV}O$ molecules containing the ^{Me,H}Pytacn ligand, $[Fe^{IV}O(^{Me,H}Pytacn)(S)]^{2+}$,[10] are required to desaturate one molecule of 9,10-dihydroanthracene (DHA), thereby yielding two molecules of the corresponding Fe^{III} species and one molecule of anthracene.[11] In the hydroxylation of alkanes by $[(Bn\text{-}TPEN)Fe^{IV}O]^{2+}$ (**1**) and $[(N4Py)Fe^{IV}O]^{2+}$ (**2**),[10] only low yields of Fe^{II} products but significant amounts of organic products generated by O_2 trapping of alkyl radicals ($\cdot CR_3$) were detected.[12] The

Scheme 1

A. Alkane hydroxylation by Cpd I in Cytochrome P450

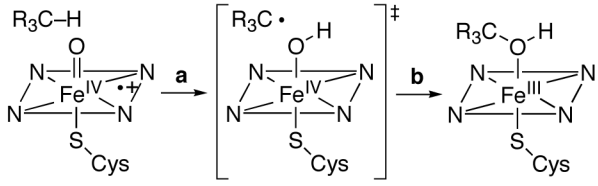

B. C-H bond activation by nonheme $Fe^{IV}O$ species

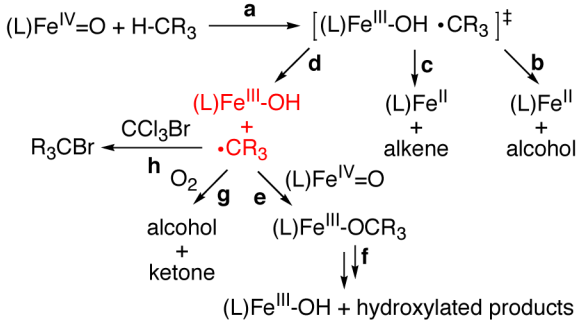

Received: August 21, 2012

   dx.doi.org/10.1021/ja308290r | J. Am. Chem. Soc. XXXX, XXX, XXX–XXX

latter result implies that the substrate radical appears to escape from the cage (Scheme 1B, pathway d) and hence reacts with O_2 instead of rebounding (Scheme 1B, pathway g). Calculations on C−H activation of cyclohexane (*c*-Hex) by **2** indicate that while the rebound barrier is as low as 1.9 kcal/mol (ΔG in solvent), the dissociation pathway is much more preferred on the free energy scale.[9b] We also recently showed that analogous reactions with non-heme $Mn^{IV}O$ complexes lead to final products containing Mn^{III}, not Mn^{II}, despite the formation of significant amounts of hydroxylated products.[13] An alternative mechanism for the $Mn^{IV}O$ reactions was therefore proposed, in which a substrate radical dissociates and reacts with a second $Mn^{IV}O$ molecule to give the corresponding Mn^{III} species and hydroxylated products (analogous to Scheme 1B, pathways e and f). Hence, there is mounting evidence in the literature that the oxygen rebound and desaturation processes may not be universal in C−H bond activation reactions by high-valent metal−oxo intermediates.

Herein we report a combination of theoretical and experimental evidence that hydroxylation of alkanes by synthetic non-heme $Fe^{IV}O$ complexes does not follow the conventional oxygen rebound and desaturation mechanisms (Scheme 1B, pathways b and c). Instead, dissociation of the substrate radical formed via hydrogen abstraction from the alkane C−H bond by $Fe^{IV}O$ species (Scheme 1B, pathway d) is shown to be more favorable than the oxygen rebound and desaturation processes in non-heme iron model reactions.

Theoretical Calculations. We investigated the C−H bond activation of *c*-Hex by the two non-heme $Fe^{IV}O$ complexes **1** and **2** using density functional theory (DFT).[14] We calculated the energy barriers for the rebound, desaturation, and dissociative processes (Scheme 1B, pathways b−d). Although similar calculations for **2** using a different computational procedure were presented previously,[9b] the ones presented here were performed to ensure that the methodology would be comparable to that used for **1**. The values discussed here are electronic energies only, calculated at the B3LYP/LACV3P^{*+}//LACVP level including CPCM solvation. The calculated free energies (ΔG) are reported in the Supporting Information (SI) only, as those values are deemed less reliable in solvent-optimized systems[15] (see the SI for more details on methodology).

Figure 1 shows the calculated energy profiles of the reactions. Apart from the initial reactant state, which has an $S = 1$ ground state, we found that singlet and triplet energies along the reaction path were high enough to not matter for the current study (see Tables S1−S4 in the SI). Hence, the energy values mentioned below are for the quintet ($S = 2$) states (relative to the triplet reactant state), unless stated otherwise. The lower energies on the quintet surface follow well-established patterns shown by many non-heme synthetic $Fe^{IV}O$ species.[7e,16] This is due to exchange-enhanced reactivity (EER), where the added electron from the substrate goes into the σ_z^* orbital of the $Fe^{IV}O$ moiety, strengthening the stabilizing exchange interactions with the other unpaired electrons.[17] This of course assumes a spin-inversion probability of unity, which may or may not be correct;[18] however, our final conclusions would not change even if singlet and triplet energies were used (see Tables S3 and S4).

The relative energies for the C−H activation transition states (TS_{C-H}) were found to be the highest ones in the whole reaction landscape (Figure 1), in accord with earlier findings that C−H bond activation by the iron−oxo complex is the rate-determining step.[6,7a] The barriers for **1** (14.2 kcal/mol) and **2** (19.1 kcal/mol) indicate that the former is more reactive, in agreement with previous experimental results.[6,18] The rebound transition states

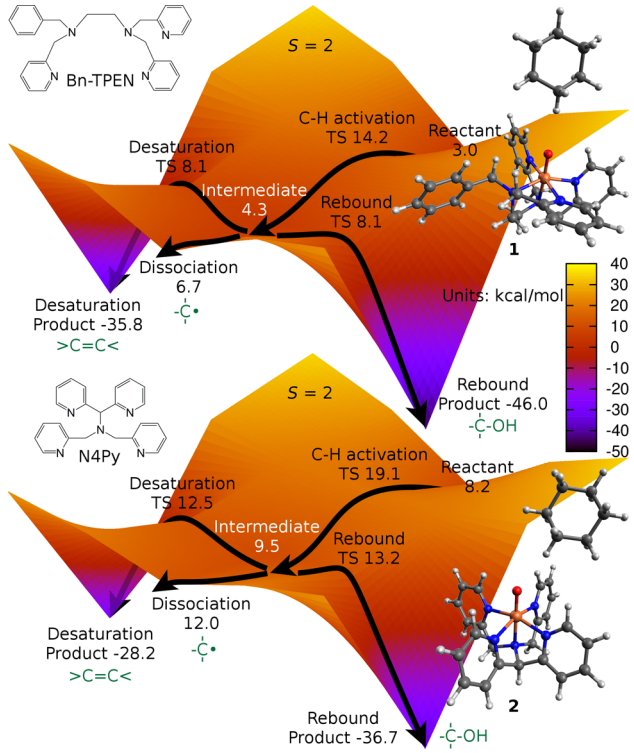

Figure 1. B3LYP/LACV3P^{*+}//LACVP-calculated energies for the reactions of (top) **1** and (bottom) **2** with *c*-Hex. Only the quintet surfaces are shown, with all values in kcal/mol relative to the triplet reactant state. Singlet and triplet values are given in the SI.

(TS_{reb}) were found to be at 8.1 and 13.2 kcal/mol for **1** and **2**, respectively, and the desaturation transition states (TS_{des}) were found to be quite comparable to the rebound barriers (i.e., 8.1 and 12.5 kcal/mol, respectively). Hence, a competition between these two follow-up reactions would be expected to occur. What is interesting here is that both TS_{reb} and TS_{des} lie higher than the system energy when the substrate radical has dissociated from the $Fe^{III}OH$ complex (i.e., E_{dis} = 6.7 and 12.0 kcal/mol for **1** and **2**, respectively). While the electronic energy differs from the other barriers by less than 2 kcal/mol, the entropy increase during dissociation should increase this difference further. The dissociation of the $Fe^{III}OH$ intermediate from the substrate radical is analogous to the proposed $Mn^{III}OH$ case[13] and is in agreement with earlier experimental[12] and theoretical findings.[9b] Hence, it is plausible to propose that dissociation of the substrate radical could be competitive with or even preferable to the rebound and desaturation pathways. To test this proposal, we performed the required C−H activation experiments with the synthetic non-heme $Fe^{IV}O$ complexes and analyzed the iron (i.e., Fe^{II} vs Fe^{III}) and organic products formed in these reactions.

Experimental Evidence. The C−H bond activation of hydrocarbons by **1** and **2** was performed with various substrates such as DHA, 1,4-cyclohexadiene (CHD), triphenylmethane (TPM), ethylbenzene (EB), and *c*-Hex. Upon addition of EB to **1** at 25 °C, **1** disappeared completely, but $[Fe^{II}(Bn\text{-}TPEN)]^{2+}$ was formed in only ~10% yield (Figure 2a; see Figure S1 in the SI for UV−vis spectra of $[Fe^{II}(Bn\text{-}TPEN)]^{2+}$ and **1**). Interestingly, addition of ferrocene (Fc) to the resulting solution caused the full formation of $[Fe^{II}(BnTPEN)]^{2+}$ and the formation of Fc^+ in ~90% yield (Figure 2a). Spectroscopic analyses of the reaction solutions were done with electron paramagnetic resonance (EPR) spectroscopy and electrospray ionization mass spectrom-

dx.doi.org/10.1021/ja308290r | J. Am. Chem. Soc. XXXX, XXX, XXX−XXX

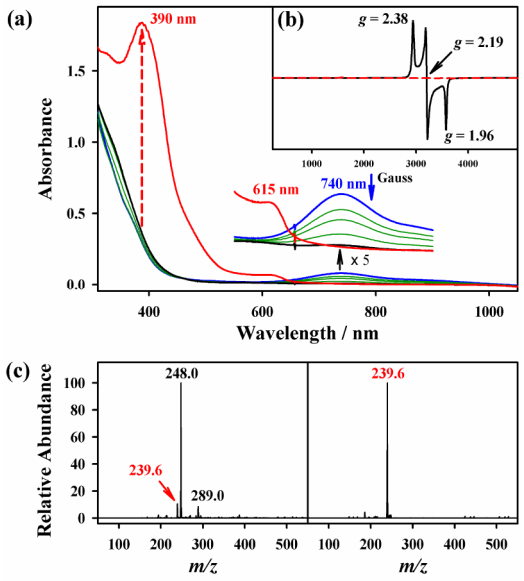

Figure 2. (a) UV−vis spectral changes observed in the reaction of **1** (2.0 mM) and EB (1.0×10^2 mM) in CH_3CN at 25 °C followed by addition of Fc (10 mM) to the resulting solution (**1**, blue line; **1** + EB, black line; **1** + EB + Fc, red line). The inset is an expansion of the 550−900 nm region showing the spectral changes of Fc^+ at 615 nm and **1** at 740 nm. The amounts of $[Fe^{II}(Bn\text{-}TPEN)]^{2+}$ at 390 nm and Fc^+ at 615 nm were calculated using ε values of 9200 and 400 M^{-1} cm^{-1} for $[Fe^{II}(Bn\text{-}TPEN)]^{2+}$ and Fc^+, respectively. (b) X-band EPR spectra recorded at 5 K with the reaction solutions of **1** + EB (black solid line) and **1** + EB + Fc (red dashed line). (c) ESI-MS spectra recorded with the reaction solutions of (left) **1** + EB and (right) **1** + EB + Fc.

etry (ESI-MS). An X-band EPR spectrum of the reaction solution of **1** and EB exhibited signals at g = 2.38, 2.19, and 1.96 (Figure 2b), characteristic of a low-spin ($S = {}^1/_2$) Fe^{III} species, whereas the ^1H NMR Evans method[19] at room temperature suggested an $S = {}^5/_2$ spin state. Upon addition of Fc to the resulting solution, the EPR spectrum became silent (Figure 2b), indicating reduction of the Fe^{III} species to an Fe^{II} species. In ESI-MS experiments, we observed ion peaks at m/z 248.0 and 289.0 in the reaction solution of **1** and EB (Figure 2c, left panel); the peaks correspond to $[Fe^{III}(OH)(Bn\text{-}TPEN)]^{2+}$ (calcd m/z 248.0) and $[Fe^{III}(OH)(Bn\text{-}TPEN)(CH_3CN)_2]^{2+}$ (calcd m/z 289.0). Reduction of the Fe^{III} species by Fc afforded an ESI-MS spectrum showing a prominent ion peak at m/z 239.6, corresponding to $[Fe^{II}(Bn\text{-}TPEN)]^{2+}$ (calcd m/z 239.5) (Figure 2c, right panel). On the basis of these analyses of the reaction solutions, we conclude that an Fe^{III} species, not an Fe^{II} species, was formed as the major product in the oxidation of EB by **1**. It should also be mentioned that the formation of Fe^{III} species was a common feature in the C−H bond activation of hydrocarbons by non-heme $Fe^{IV}O$ complexes, irrespective of the iron complex (i.e., **1** or **2**) and the organic substrate (i.e., DHA, CHD, TPM, EB, or *c*-Hex) (see Figures S2 and S3 for data from the **1** + *c*-Hex and **2** + EB reactions, respectively).[20] Furthermore, it is worth noting that the amounts of Fe^{II} and Fe^{III} products varied slightly depending on the substrate (Table S13) but not on the $Fe^{IV}O$ complex and substrate concentrations (see Figures S4 and S5 for the reactions of EB with **1** and **2**, respectively). Finally, we ruled out the possibility that the Fe^{III} species was produced by a comproportionation reaction between $Fe^{IV}O$ and Fe^{II} species. For example, when we mixed equal amounts of **2** and $[Fe^{II}(N4Py)]^{2+}$ under the conditions of the C−H bond activation reaction (i.e., in CH_3CN at 25 °C), the reactants remained intact and the formation of an Fe^{III} species (i.e., $[Fe^{III}(OH)(N4Py)]^{2+}$) was not observed (Figure S6). This result demonstrates that the Fe^{III} species is formed via the dissociation mechanism (Scheme 1B, pathway d) rather than a comproportionation reaction between $Fe^{IV}O$ and Fe^{II} species. A similar conclusion was reached in the C−H bond activation reaction of hydrocarbons by non-heme $Mn^{IV}O$ species.[13,21]

Product analysis revealed that products formed in the C−H bond activation reactions by non-heme $Fe^{IV}O$ complexes depended on the reaction conditions, such as the presence of O_2 or an alkyl radical scavenger (i.e., CCl_3Br) (see the Experimental Section in the SI). For example, cyclohexanol (25 ± 2%) and cyclohexanone (11 ± 2%) were obtained as products in the reaction of **1** (2.0 mM) and *c*-Hex (1.0×10^3 mM) under an Ar atmosphere in CH_3CN at 25 °C. An isotope experiment with ^{18}O-labeled **1** (**1**-^{18}O) showed that the oxygens in the cyclohexanol and cyclohexanone products were derived from **1** (Figure S7). When the identical reaction was carried out with **1**-^{18}O in the presence of $^{16}O_2$, the product distribution was different [i.e., cyclohexanol (10 ± 2%) and cyclohexanone (21 ± 3%)] and the cyclohexanol product contained both ^{16}O (77 ± 6%) and ^{18}O (23 ± 3%) (Figure S7). In addition, when we carried out hydroxylations of *c*-Hex using **1** and **2** in the presence of CCl_3Br under an Ar atmosphere, we observed the formation of bromocyclohexane as the sole product, indicating that a cyclohexanyl radical was trapped by CCl_3Br.[3c,22] The experimental evidence provided here strongly supports the proposal that C−H bond activation by non-heme $Fe^{IV}O$ complexes prefers the dissociation process (Scheme 1B, pathway d) rather than the oxygen rebound and desaturation processes (Scheme 1B, pathways b and c).

Comparison to Heme Systems. As shown above, the substrate dependence of the second barrier determines the precise nature of the products formed.[9a] As our TS_{reb} is less than 2 kcal/mol higher than E_{dis} (disregarding entropy), it is not excluded that certain substrates will more easily rebound/desaturate than others. With a given substrate and otherwise identical conditions, however, we can make some interesting comparisons between heme and non-heme $Fe^{IV}O$ systems. In our example using *c*-Hex, calculations showed that the rebound reaction occurs over a very low TS_{reb} in the low-spin heme case,[23] with which few other reactions, including the dissociation reaction, could compete. In the non-heme case, the rebound reaction would occur in the high-spin state with a barrier that is small but nevertheless larger than the dissociation barrier. The question is therefore "Why does TS_{reb} lie lower in the heme case?"

There may be several factors that could produce an energy difference of this scale. Among these, we observed two plausible ones in our calculations. Figure 3 shows the valence-electron orbitals in the heme $Fe^{IV}OH$ intermediate stage versus the non-heme $Fe^{III}OH$ stage. In heme, the low-spin configuration is preferred, and the second electron is transferred to a low-lying orbital (π^*_{yz}). Therefore, this process would not be expected to contribute much to any barrier.[2b,23] In non-heme cases, the situation is somewhat similar, with the second electron being transferred to π^*_{yz} as well, even though the system is in a high-spin state.[9a] This has one drawback compared with the heme case. The number of favorable exchange interactions between the five unpaired electrons in a non-heme high-spin $Fe^{III}OH$ configuration is diminished by 40% upon loss of the radical at π^*_{yz}, presumably contributing to a barrier. The other factor is steric effects due to substrate and/or ligand bulkiness. In the high-spin

dx.doi.org/10.1021/ja308290r | J. Am. Chem. Soc. XXXX, XXX, XXX−XXX

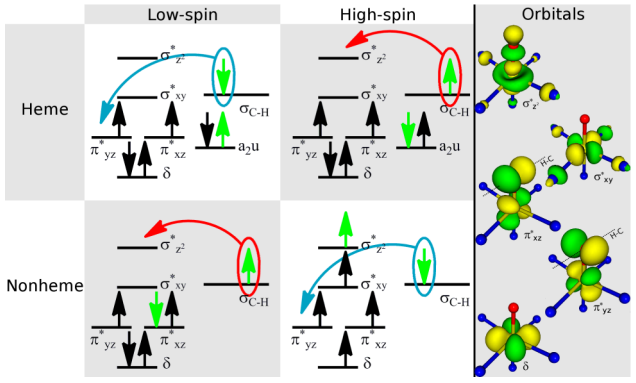

Figure 3. Valence-electron orbitals involved in electron shifts during the rebound step for (top) heme ($Fe^{IV}OH$) and (bottom) non-heme ($Fe^{III}OH$) intermediates. Blue arrows indicate the energetically preferred reactions, while red arrows generally lead to higher barriers. Green spin arrows indicate electrons nascent from the substrate. See the text for a detailed discussion.

non-heme case, the Fe−O−C angle is very roughly 180° as a result of the selection rules of TS_{C-H},[7a] but the substrate must relocate to assume a more bent angle in order to interact with the π^*_{yz} orbital in the second electron movement step (this relocation is not necessary for the low-spin heme case). Hence, we suggest that a difference in EER and steric effects are the two main factors responsible for the difference between heme and non-heme cases.

In conclusion, theoretical calculations have predicted that dissociation of the substrate radicals formed by hydrogen abstraction from alkane C−H bonds by non-heme $Fe^{IV}O$ complexes is more favorable than the oxygen rebound and desaturation processes. This is in contrast to the case of heme $Fe^{IV}O$, where the low-spin, reorientation-free, and EER-independent reactions lead to a minimal rebound barrier. This theoretical prediction has been verified by experimental results obtained by analyzing the products formed in C−H bond activation of various substrates by synthetic non-heme $Fe^{IV}O$ complexes. Thus, the general view that C−H bond activation by high-valent metal−oxo species universally occurs via the hydrogen abstraction/oxygen rebound mechanism should be viewed with caution.

■ ASSOCIATED CONTENT

Supporting Information

Theoretical and experimental methods and additional data. This material is available free of charge via the Internet at http://pubs.acs.org.

■ AUTHOR INFORMATION

Corresponding Author

sason@yfaat.ch.huji.ac.il; wwnam@ewha.ac.kr

Notes

The authors declare no competing financial interest.

[§]K.-B.C. and X.W. contributed equally.

■ ACKNOWLEDGMENTS

The research at EWU was supported by NRF/MEST of Korea through CRI, GRL (2010-00353), and WCU (R31-2008-000-10010-0) (to W.N.). S.S. acknowledges Israel Science Foundation Grant ISF 53/09 for financial support.

■ REFERENCES

(1) Nam, W. *Acc. Chem. Res.* **2007**, *40*, 465 and references therein.
(2) (a) Ortiz de Montellano, P. R. *Cytochrome P450: Structure, Mechanism, and Biochemistry*; Kluwer/Plenum: New York, 2005. (b) Shaik, S.; Kumar, D.; de Visser, S. P.; Altun, A.; Thiel, W. *Chem. Rev.* **2005**, *105*, 2279. (c) Ortiz de Montellano, P. R. *Chem. Rev.* **2010**, *110*, 932. (d) Rittle, J.; Green, M. T. *Science* **2010**, *330*, 933.
(3) (a) Groves, J. T.; McClusky, G. A. *J. Am. Chem. Soc.* **1976**, *98*, 859. (b) Groves, J. T.; Van Der Puy, M. *J. Am. Chem. Soc.* **1976**, *98*, 5290. (c) Groves, J. T. *J. Chem. Educ.* **1985**, *62*, 928. (d) Groves, J. T. *Proc. Natl. Acad. Sci. U.S.A.* **2003**, *100*, 3569.
(4) (a) Ogliaro, F.; Harris, N.; Cohen, S.; Filatov, M.; de Visser, S. P.; Shaik, S. *J. Am. Chem. Soc.* **2000**, *122*, 8977. (b) Guallar, V.; Baik, M.-H.; Lippard, S. J.; Friesner, R. A. *Proc. Natl. Acad. Sci. U.S.A.* **2003**, *100*, 6998. (c) Kamachi, T.; Yoshizawa, K. *J. Am. Chem. Soc.* **2003**, *125*, 4652.
(5) (a) Krebs, C.; Galonić Fujimori, D.; Walsh, C. T.; Bollinger, J. M., Jr. *Acc. Chem. Res.* **2007**, *40*, 484. (b) Que, L., Jr. *Acc. Chem. Res.* **2007**, *40*, 493. (c) Nam, W. *Acc. Chem. Res.* **2007**, *40*, 522.
(6) (a) Kaizer, J.; Klinker, E. J.; Oh, N. Y.; Rohde, J.-U.; Song, W. J.; Stubna, A.; Kim, J.; Münck, E.; Nam, W.; Que, L., Jr. *J. Am. Chem. Soc.* **2004**, *126*, 472. (b) Seo, M. S.; Kim, N. H.; Cho, K.-B.; So, J. E.; Park, S. K.; Clémancey, M.; Garcia-Serres, R.; Latour, J.-M.; Shaik, S.; Nam, W. *Chem. Sci.* **2011**, *2*, 1039.
(7) (a) Hirao, H.; Kumar, D.; Que, L., Jr.; Shaik, S. *J. Am. Chem. Soc.* **2006**, *128*, 8590. (b) de Visser, S. P. *J. Am. Chem. Soc.* **2006**, *128*, 9813. (c) Comba, P.; Maurer, M.; Vadivelu, P. *J. Phys. Chem. A* **2008**, *112*, 13028. (d) Hirao, H.; Que, L., Jr.; Nam, W.; Shaik, S. *Chem.—Eur. J.* **2008**, *14*, 1740. (e) Geng, C.; Ye, S.; Neese, F. *Angew. Chem., Int. Ed.* **2010**, *49*, 5717.
(8) (a) Broun, P.; Shanklin, J.; Whittle, E.; Somerville, C. *Science* **1998**, *282*, 1315. (b) Whittle, E. J.; Tremblay, A. E.; Buist, P. H.; Shanklin, J. *Proc. Natl. Acad. Sci. U.S.A.* **2008**, *105*, 14738. (c) Mukherjee, A.; Martinho, M.; Bominaar, E. L.; Münck, E.; Que, L., Jr. *Angew. Chem., Int. Ed.* **2009**, *48*, 1780. (d) Bigi, M. A.; Reed, S. A.; White, M. C. *Nat. Chem.* **2011**, *3*, 216.
(9) (a) Usharani, D.; Janardanan, D.; Shaik, S. *J. Am. Chem. Soc.* **2011**, *133*, 176. (b) Janardanan, D.; Usharani, D.; Chen, H.; Shaik, S. *J. Phys. Chem. Lett.* **2011**, *2*, 2610.
(10) Abbreviations: ^{Me,H}Pytacn = 1-(2′-pyridylmethyl)-4,7-dimethyl-1,4,7-triazacyclononane; Bn-TPEN = *N*-benzyl-*N*,*N*′,*N*′-tris(2-pyridylmethyl)ethane-1,2-diamine; N4Py = *N*,*N*-bis(2-pyridylmethyl)-*N*-bis(2-pyridyl)methylamine.
(11) Company, A.; Prat, I.; Frisch, J. R.; Mas-Ballesté, R.; Güell, M.; Juhász, G.; Ribas, X.; Münck, E.; Luis, J. M.; Que, L., Jr.; Costas, M. *Chem.—Eur. J.* **2011**, *17*, 1622.
(12) Klinker, E. J. Ph.D. Thesis, University of Minnesota, Minneapolis, MN, 2007.
(13) Wu, X.; Seo, M. S.; Davis, K. M.; Lee, Y.-M.; Chen, J.; Cho, K.-B.; Pushkar, Y. N.; Nam, W. *J. Am. Chem. Soc.* **2011**, *133*, 20088.
(14) Kohn, W.; Sham, L. J. *Phys. Rev.* **1965**, *140*, A1133.
(15) (a) Ho, J.; Klamt, A.; Coote, M. L. *J. Phys. Chem. A* **2010**, *114*, 13442. (b) Cho, K.-B.; Chen, H.; Janardanan, D.; de Visser, S. P.; Shaik, S.; Nam, W. *Chem. Commun.* **2012**, *48*, 2189.
(16) Ye, S.; Neese, F. *Proc. Natl. Acad. Sci. U.S.A.* **2011**, *108*, 1228.
(17) Shaik, S.; Chen, H.; Janardanan, D. *Nat. Chem.* **2011**, *3*, 19.
(18) Cho, K.-B.; Kim, E. J.; Seo, M. S.; Shaik, S.; Nam, W. *Chem.—Eur. J.* **2012**, *18*, 10444.
(19) Evans, D. F.; Jakubovic, D. A. *J. Chem. Soc., Dalton Trans.* **1988**, 2927. The measured magnetic moment was 5.7μ_B, implying an $S = {}^5/_2$ state.
(20) The reactions of **2** with DHA and CHD reached completion within several seconds. In addition, the observed rate constant for the reaction of **2** with EB was 2.2×10^{-3} s^{-1} (Figure S3).
(21) Cho, K.-B.; Shaik, S.; Nam, W. *J. Phys. Chem. Lett.* **2012**, *3*, 2851.
(22) Groves, J. T.; Nemo, T. E. *J. Am. Chem. Soc.* **1983**, *105*, 6243.
(23) Lai, W.; Chen, H.; Cohen, S.; Shaik, S. *J. Phys. Chem. Lett.* **2011**, *2*, 2229.